



Suppression of Walker breakdown in magnetic domain wall propagation through structural control of spin wave emission

David M. Burn and Del Atkinson

Citation: [Applied Physics Letters](#) **102**, 242414 (2013); doi: 10.1063/1.4811750

View online: <http://dx.doi.org/10.1063/1.4811750>

View Table of Contents: <http://scitation.aip.org/content/aip/journal/apl/102/24?ver=pdfcov>

Published by the [AIP Publishing](#)

Articles you may be interested in

[Spin wave based parallel logic operations for binary data coded with domain walls](#)

J. Appl. Phys. **115**, 17D505 (2014); 10.1063/1.4863936

[Spin-wave excitations induced by spin current through a magnetic point contact with a confined domain wall](#)

Appl. Phys. Lett. **101**, 092405 (2012); 10.1063/1.4745777

[Fast domain wall dynamics in magnetic nanotubes: Suppression of Walker breakdown and Cherenkov-like spin wave emission](#)

Appl. Phys. Lett. **99**, 122505 (2011); 10.1063/1.3643037


[Spin wave assisted current induced magnetic domain wall motion](#)

Appl. Phys. Lett. **96**, 242501 (2010); 10.1063/1.3446833

[Magnetic domain-wall motion by propagating spin waves](#)


Appl. Phys. Lett. **94**, 112502 (2009); 10.1063/1.3098409

Agilent's Electronic Measurement Group is becoming **Keysight Technologies**.



Engineering Education & Research Resources DVD 2014

Agilent is the key to your test and measurement needs **Order yours**



Suppression of Walker breakdown in magnetic domain wall propagation through structural control of spin wave emission

David M. Burn and Del Atkinson^{a)}

Department of Physics, Durham University, Durham DH1 3LE, United Kingdom

(Received 7 March 2013; accepted 6 June 2013; published online 21 June 2013)

The control of individual magnetic domain walls has potential for future spintronic memory and data processing applications. The speed and reliability of such devices are determined by the dynamic properties of the domain walls. Typically, spin precession limitations lead to Walker breakdown, limiting wall velocity resulting in low mobility. Here, we show the suppression of Walker breakdown by the careful design of small amplitude periodic nanowire structuring to match the periodicity of domain wall spin structure transformations. This opens up a channel for energy dissipation via spin wave emission, allowing a domain wall to maintain its spin structure during propagation. © 2013 AIP Publishing LLC. [<http://dx.doi.org/10.1063/1.4811750>]

Magnetic domain wall (DW) motion is significant in wide ranging applications, from spintronic technologies for data storage,¹ processing,² and sensing applications³ to the manipulation of atoms⁴ and nanoparticles⁵ for nanoassembly or nanodelivery. Typically, DW velocity increases linearly with field^{3,6} up to the Walker field, where periodic transformations of the DW spin structure results in a dramatic reduction in time-averaged DW velocity, known as Walker breakdown.^{7,8} This limits operation speeds and functional performance in both nanowires⁹ and thin films.¹⁰

For device applications, fast DW motion over a broad field range with constant or monotonic field-dependent velocity is desirable and various approaches have attempted to achieve this by suppressing DW breakdown behavior. Applying additional fields, either quasi-static perpendicular fields^{11,12} or oscillating axial fields,¹³ is one approach, but they add technical complexity in both the device architecture and control protocol. Alternatively, modified nanowire designs incorporating either magnetic underlayers¹⁴ to intrinsically supply a bias field or large-scale lateral comb structures¹⁵ to repeatedly reset the DW structure show improved DW dynamics, but both approaches add fabrication complexity and in the latter case significantly reduce device packing density. In contrast, nanowire edge roughness has shown improved DW dynamics by distorting the vortex core nucleation process at the nanowire edges.^{16,17} The removal of the edges in simulations by forming tubular nanowires with periodic boundaries has shown improved DW dynamics,^{18,19} however, the geometrical complexity of tubular nanostructures is incompatible with conventional nanoscale lithographic fabrication, and therefore this approach is not suitable as a mode of control for technological applications.

Here, we demonstrate the suppression of Walker breakdown by the inclusion of small amplitude structural modulation to a planar nanowires' geometry by careful matching of the modulation wavelength to the periodic length-scale of the DW structural transformations. This small amplitude structuring would not significantly affect the packing density but does make a significant improvement to the DW dynamics,

by opening up a channel for the dissipation of DW energy via spin wave emission that disrupts the DW transformation process.

Previous studies with periodic rectangular anti-notches¹⁵ and triangular or sinusoidal edge modifications²⁰ show modified DW dynamics,²¹ but critically the linkage between the Walker breakdown periodicity and wire structuring wavelength has not been explored and the mechanism for suppressing Walker breakdown with periodic modulation has not been elucidated. This paper presents a detailed systematic micromagnetic investigation^{22,23} of the dynamic behavior of DWs and shows how Walker breakdown suppression can be achieved by careful manipulation of nanowire edge modulation parameters.

Planar nanowires with average width of 250 nm were modified by the introduction of small amplitude sinusoidal edge modulations characterized by their wavelength and amplitude as illustrated in Figure 1(j). The DW velocity in these structures was investigated as a function of applied field. For an un-modulated wire structure (Figures 1(a)–1(e)), the velocity increases linearly with field up to the Walker field where the drop in time-averaged DW velocity results from Walker breakdown. Further increases in field bring about an increase in velocity but show complex behavior resulting from multiple breakdown events.

During Walker breakdown, transitions between transverse wall (Figure 1(a)) and vortex core (Figure 1(b)) micromagnetic structures take place with a spatial periodicity shown by the open squares in Figure 1(e) and occur in this case with a minimum periodicity of 0.5 μm . This periodicity is dependent upon the material properties such as the Gilbert damping parameter, α , the saturation magnetisation, M_s , and the exchange stiffness constant, A .

At an edge modulation wavelength of $\lambda = 0.4 \mu\text{m}$, below the periodicity of DW structural changes, the effect of modulation amplitude on the DW motion can be studied. With 15 nm amplitude edge modulation (Figure S1²³), fast DW motion is observed at low fields, but at higher fields, the motion is interrupted by breakdown events resulting from complex DW dynamics. However, by increasing the amplitude to 25 nm (Figure 1(j)), the behavior changes and critically the breakdown

^{a)}Electronic mail: del.atkinson@durham.ac.uk

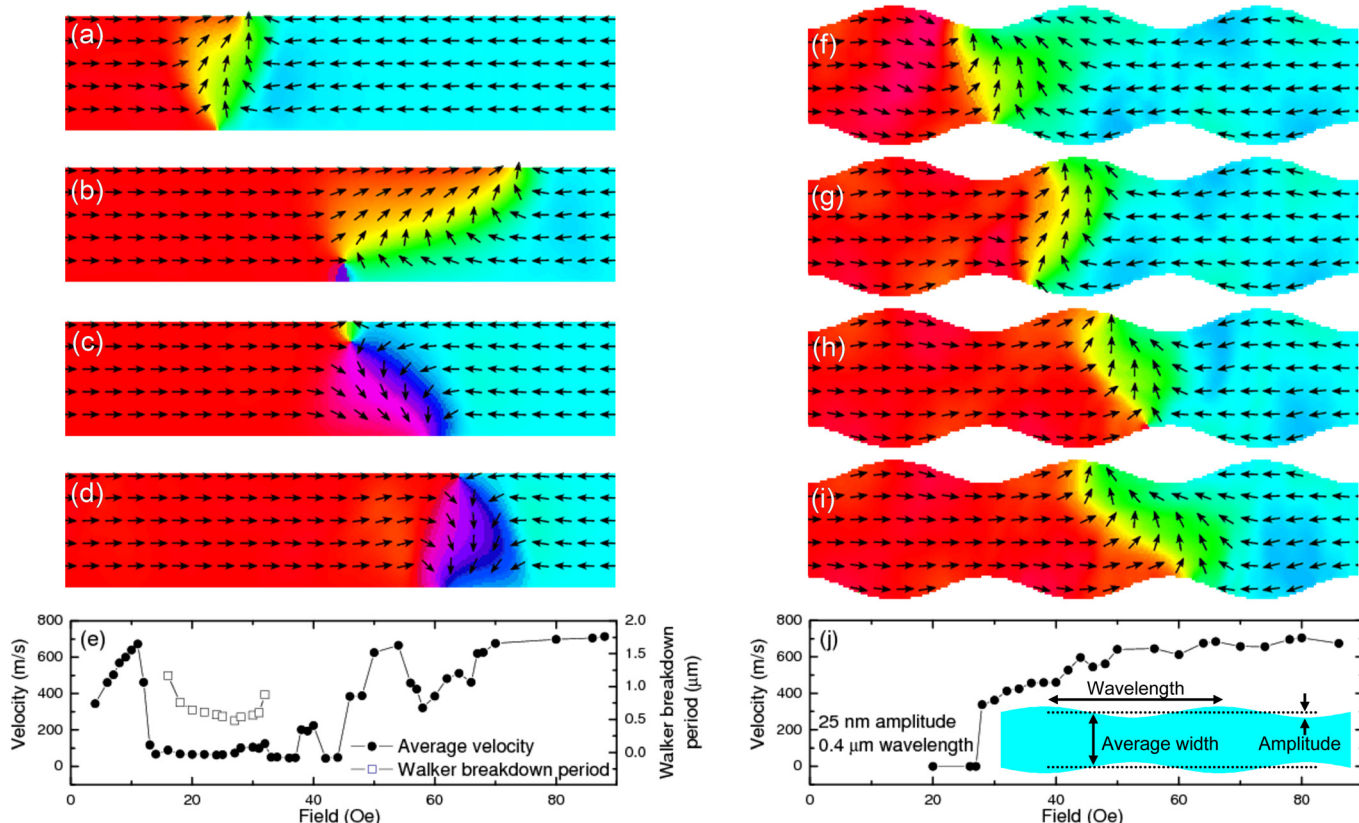


FIG. 1. DW propagation at 30 Oe in a 250 nm wide (a)–(d) un-modulated and (f)–(i) modulated nanowire with 25 nm amplitude and 0.4 μm wavelength. (e) and (j) show the average DW velocity for these structures where Walker breakdown occurs in the plain wire with the periodicity shown by the open squares.

events are suppressed and high DW velocity is maintained over a wide field range, starting below the Walker breakdown field experienced in the un-modulated wire. The structural modulation increases the de-pinning field compared to un-modulated structures, which for optimal device operation must be controlled and minimized in order to maximize the functional field range.

A phase diagram showing the field dependence DW velocity as a function of structural wavelength, λ , is shown in Figure 2(b), for $\lambda = 0.2 \mu\text{m}$ to $0.8 \mu\text{m}$ with an amplitude of 25 nm and can be compared with the field dependent velocity behavior for the un-modulated wire 2(a). The wavelength of the edge modulation has a significant effect on the dynamic properties, with several regions of different behavior appearing on the diagram showing complex DW dynamics, suppression of Walker breakdown and pinning of DWs.

At low fields, the DWs are pinned, showing no dynamic behavior up to the de-pinning field. This field depends on the structural wavelength and shows a $1/\lambda$ dependence on the modulation, indicated by the solid line in Figure 2(b). An increase in de-pinning field such as this can result from a reduction of axial anisotropy due to wire modulation²¹ or increasing edge roughness.¹⁷

Above the de-pinning field, the DW dynamics depend strongly upon the modulation wavelength. For longer wavelength modulation, $\lambda > 0.5 \mu\text{m}$, complex dynamic behavior occurs that includes additional suppression of Walker breakdown but over a limited field range. In contrast, for λ below $0.5 \mu\text{m}$, the DW velocity rises rapidly above the de-pinning field, becoming largely field invariant at higher fields. Here,

the DW motion is consistent, where the transverse structure is maintained and only small variations in the velocity occur due to stretching and compressing of the domain wall as it propagates through the modulated structure.

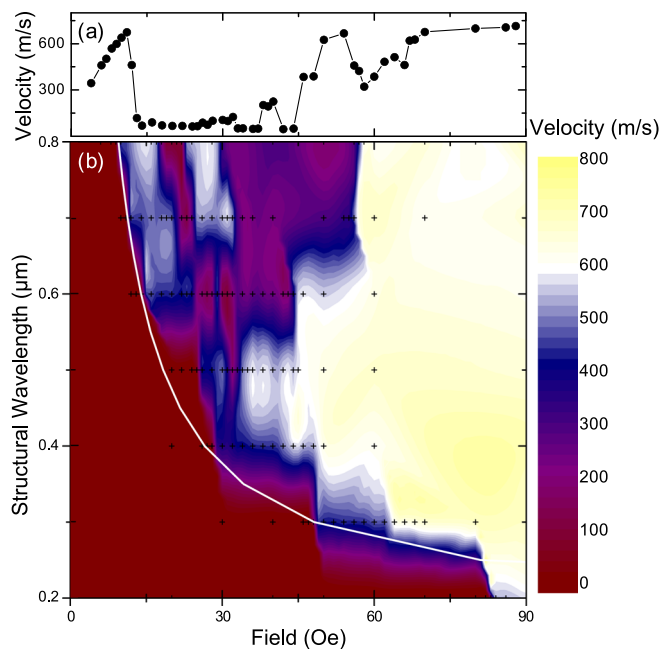


FIG. 2. (a) DW velocity as a function of applied field for a un-modulated 250 nm wide wire. (b) Phase diagram showing DW velocity as a function of edge modulation wavelength for a 250 nm wide wire with 25 nm amplitude modulations. The white line indicates a $1/\lambda$ fit to the de-pinning field and the points represent the simulation conditions that have been investigated.

This phase diagram shows that the edge modulation wavelength can control how DW propagation will be affected by Walker breakdown. Comparing Figures 2(a) and 2(b) shows how the edge modulation can improve the dynamic properties of DW propagation where high velocity can be achieved for conditions where Walker breakdown would occur in the un-modulated wire.

The key to understanding and controlling Walker breakdown is the physical mechanism for the transition between transverse and vortex core wall states. Suppression of breakdown of a propagating DW results from disruption of the periodic DW structure transformations by the periodic edge modulation. Magnetostatic effects make transverse walls more energetically favorable in narrower wires and vortex walls more favorable in wider wires.^{24,25} In the edge modulated nanowires, there is a spatial dependence to the effective wire width that gives rise to variations in the energy landscape for the DW as it propagates the wire. The influence of the modulation on DW energy and thus suppression of Walker breakdown is then also to be expected to depend upon the amplitude, as mentioned earlier. Analysis here shows that Walker breakdown is more reliably suppressed with larger amplitude modulation. The propagation of a transverse wall leads to the development of an increasing out-of-plane component of magnetic moment and it is the development of this component that initiates the transition from transverse to vortex core structure. Therefore, controlling the growth of this out-of-plane component of DW magnetization is key to suppressing Walker breakdown.

When the modulation wavelength is larger than the vortex core nucleation period, the vortex core forms prior to the wall interaction with a constriction in the nanowire geometry. As the modulation wavelength is reduced below the periodicity of vortex core nucleation, the transformation is prevented at the point where the vortex core would otherwise have nucleated. Therefore, when the structural modulation wavelength is shorter than the vortex core nucleation period, a DW arrives at a constriction before the vortex core can fully form, maintaining the transverse structure and allowing the DW to continue at high velocity. Thus, Walker breakdown is suppressed, giving rise to a field regime with fast DW motion in a region that would have experienced Walker breakdown without structural modulation.

The mechanism for suppression is most readily explained by considering a modulated structure with a wavelength $\lambda = 0.8 \mu\text{m}$ and an amplitude of 25 nm, which experiences all regimes of DW dynamics at different fields. Below 16 Oe, the DW motion shows uniform propagation behavior, by 18 Oe the wall motion displays Walker breakdown and around 24 Oe Walker breakdown is suppressed. Analysis of the time evolution of the out-of-plane component of magnetization, M_z , as a function of position along the wire axis is shown for each of the three field amplitudes in Figure 3. The peaks in M_z show the position of the DW and the movement of this peak in time shows the DW motion along the wire. The insets in each panel show snapshots of the DW structure at the 200 ps position and further images showing the time evolution of the DW structure can be found in Figure S2.²³

At 16 Oe (Figure 3(a)), the DW has high velocity in the x direction and a stable M_z component that does not develop

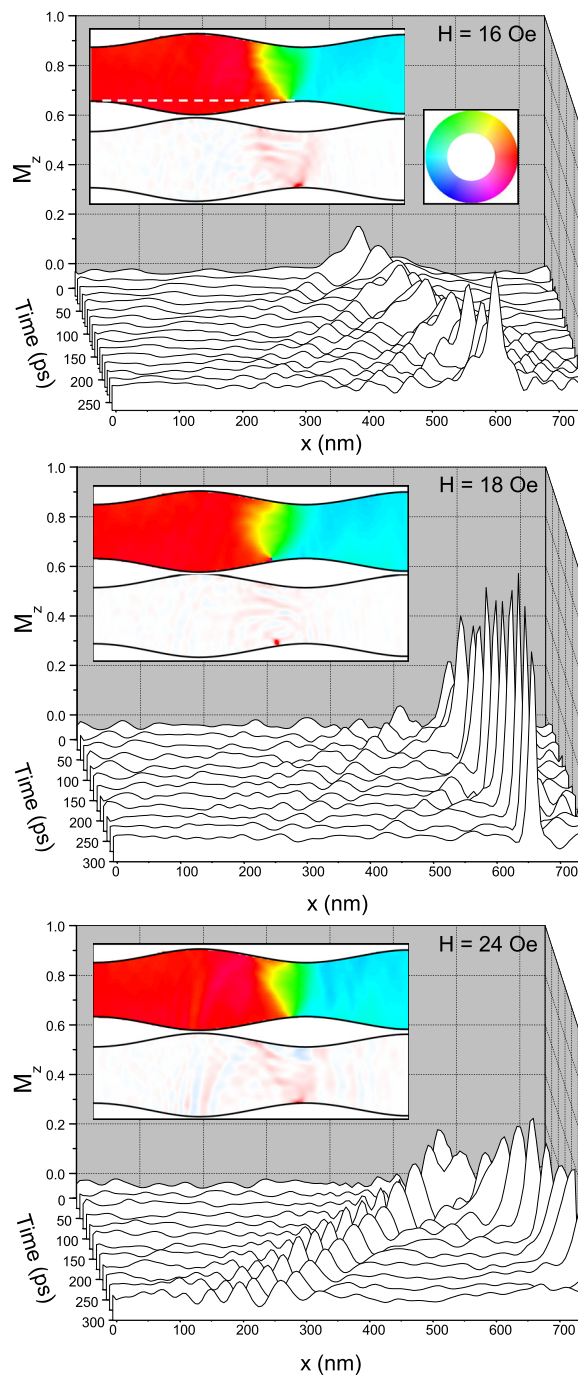


FIG. 3. Time evolution of M_z as a function of position along the nanowire shown for 16 Oe, 18 Oe, and 24 Oe. At 24 Oe, the M_z disturbance ejects a spin wave leading to Walker breakdown suppression. The x - y angle of the spins indicated by the colour wheel is shown in the top inset and M_z is shown in the bottom inset. The y position for the graphs is indicated by the dashed line in the inset.

sufficiently to nucleate a vortex core, so the DW propagates consistently. In contrast, at 18 Oe (Figure 3(b)), a large M_z component is associated with the development of a vortex core at the edge of the nanowire as the wall approaches the constriction in the wire. The vortex core propagates through the constriction and continues to traverse the wire, leading into Walker breakdown. Figure 3(c) shows the effect of a further increase in field up to 24 Oe; in this case, a vortex core nucleates at the edge in the wider section, propagates towards the narrower section, where it is annihilated on the

same side of the wire with the emission of a spin wave that travels in the negative x direction. The spin wave carries away magnetostatic energy from the DW so that the remaining M_z component of the wall remains as a disturbance of the propagating transverse wall structure. The distorted DW continues to propagate at high velocity in the positive x direction without Walker breakdown. At higher fields, for $\lambda = 0.8 \mu\text{m}$, the DW propagation resumes Walker breakdown behavior as the energy loss to the spin wave is insufficient to prevent a sustained vortex. This explains the complex suppression and return of Walker breakdown shown in the field dependent velocity behavior in Figure 2. For $\lambda < 0.5 \mu\text{m}$, Walker breakdown is suppressed by this mechanism at all fields above the de-pinning field.

The interaction between spin waves and DWs can affect the DW motion by the absorption^{26–28} and emission²⁹ of spin wave energy. In the wake of a propagating DW, the loss of energy through the emission of spin waves damps the DW motion, which can stabilize fast dynamics in the limit of “huge anisotropies.”^{30,31} Here, we show that the triggering of the spin wave emission and stabilization process can be achieved in materials with negligible intrinsic anisotropy by structural modulation. Critically, by controlling the spatial synchronization of spin-wave emission with the nanowire edge modulation, consistent high velocity DW propagation behavior can be achieved.

In summary, the phenomenon of Walker breakdown in the propagation of DWs in planar nanowires can be controlled by small amplitude ($\sim 10\%$) periodic structuring. When the structural wavelength is shorter than the periodic length-scale of the wall transitions causing Walker breakdown, the breakdown is suppressed by the emission of spin waves. The comparatively small sinusoidal edge modulation has a dramatic effect on the DW dynamic properties and provides a realistic way to achieve reliable DW behavior in devices in which dense packing of these structures is possible.

We acknowledge E. Arac, L. K. Bogart, and A. T. Hindmarch for their helpful discussions. This work was supported by a grant from the EPSRC.

¹S. S. P. Parkin, M. Hayashi, and L. Thomas, *Science* **320**, 190 (2008).

²D. A. Allwood, G. Xiong, C. C. Faulkner, D. Atkinson, D. Petit, and R. P. Cowburn, *Science* **309**, 1688 (2005).

³T. Ono, H. Miyajima, K. Shigeto, K. Mibu, N. Hosoi, and T. Shinjo, *Science* **284**, 468 (1999).

⁴A. D. West, K. J. Weatherill, T. J. Hayward, P. W. Fry, T. Schrefl, M. R. J. Gibbs, C. S. Adams, D. A. Allwood, and I. G. Hughes, *Nano Lett.* **12**, 4065 (2012).

⁵G. Ruan, G. Vieira, T. Henighan, A. Chen, D. Thakur, R. Sooryakumar, and J. O. Winter, *Nano Lett.* **10**, 2220 (2010).

⁶D. Atkinson, D. A. Allwood, C. C. Faulkner, G. Xiong, M. D. Cooke, and R. P. Cowburn, *IEEE Trans. Magn.* **39**, 2663 (2003).

⁷N. L. Schryer and L. R. Walker, *J. Appl. Phys.* **45**, 5406 (1974).

⁸G. S. D. Beach, C. Nistor, C. Knutson, M. Tsoi, and J. L. Erskine, *Nature Mater.* **4**, 741 (2005).

⁹H. Tanigawa, T. Koyama, M. Bartkowiak, S. Kasai, K. Kobayashi, T. Ono, and Y. Nakatani, *Phys. Rev. Lett.* **101**, 207203 (2008).

¹⁰D. M. Burn and D. Atkinson, *J. Appl. Phys.* **108**, 073926 (2010).

¹¹K. Richter, R. Varga, G. A. Badini-Confalonieri, and M. Vazquez, *Appl. Phys. Lett.* **96**, 182507 (2010).

¹²M. T. Bryan, T. Schrefl, D. Atkinson, and D. A. Allwood, *J. Appl. Phys.* **103**, 073906 (2008).

¹³K. Weerts, W. Van Roy, G. Borghs, and L. Lagae, *Appl. Phys. Lett.* **96**, 062502 (2010).

¹⁴J.-Y. Lee, K.-S. Lee, and S.-K. Kim, *Appl. Phys. Lett.* **91**, 122513 (2007).

¹⁵E. R. Lewis Petit, D. Petit, L. O'Brien, A. Fernandez-Pacheco, J. Sampaio, A.-V. Jausovec, H. T. Zeng, D. E. Read, and R. P. Cowburn, *Nature Mater.* **9**, 980 (2010).

¹⁶Y. Nakatani, A. Thiaville, and J. Miltat, *Nature Mater.* **2**, 521 (2003).

¹⁷E. Martinez, L. Lopez-Diaz, L. Torres, C. Tristan, and O. Alejos, *Phys. Rev. B* **75**, 174409 (2007).

¹⁸M. Yan, C. Andreas, A. Kákay, F. García-Sánchez, and R. Hertel, *Appl. Phys. Lett.* **99**, 122505 (2011).

¹⁹M. Yan, A. Kákay, S. Gliga, and R. Hertel, *Phys. Rev. Lett.* **104**, 057201 (2010).

²⁰J. Ieda, H. Sugishita, and S. Maekawa, *J. Magn. Magn. Mater.* **322**, 1363 (2010).

²¹H. G. Piao, J. H. Shim, and D. Djuhana, *IEEE Trans. Magn.* **46**, 224 (2010).

²²M. J. Donahue and D. G. Porter, *OOMMF User's Guide Version 1.0*, NIST, Gaithersburg, MD (1999).

²³See supplementary material at <http://dx.doi.org/10.1063/1.4811750> for micromagnetic simulation details and additional results showing the domain wall structure and amplitude dependence.

²⁴R. D. McMichael and M. J. Donahue, *IEEE Trans. Magn.* **33**, 4167 (1997).

²⁵Y. Nakatani, A. Thiaville, and J. Miltat, *J. Magn. Magn. Mater.* **290–291**, 750 (2005).

²⁶S.-M. Seo, H.-W. Lee, H. Kohno, and K.-J. Lee, *Appl. Phys. Lett.* **98**, 012514 (2011).

²⁷Y.-Le. Maho, J.-V. Kim, and G. Tatara, *Phys. Rev. B* **79**, 174404 (2009).

²⁸D.-S. Han Kim, S.-K. Kim, J.-Y. Lee, S. J. Hermsdoerfer, H. Schultheiss, B. Leven, and B. Hillebrands, *Appl. Phys. Lett.* **94**, 112502 (2009).

²⁹X. S. Wang, P. Yan, Y. H. Shen, G. E. W. Bauer, and X. R. Wang, *Phys. Rev. Lett.* **109**, 167209 (2012).

³⁰R. Wieser, E. Y. Vedmedenko, and R. Wiesendanger, *Phys. Rev. B* **81**, 024405 (2010).

³¹D. Bouzidi and H. Suhl, *Phys. Rev. Lett.* **65**, 2587 (1990).